Biochimie 93 (2011) 806–816

Contents lists available at ScienceDirect

Biochimie

journal homepage: www.elsevier.com/locate/biochi

Research paper

Structural basis for both pro- and anti-inflammatory response induced by mannose-specific legume lectin from *Cymbosema roseum*

Bruno A.M. Rocha [a,h], Plinio Delatorre [b], Taianá M. Oliveira [a], Raquel G. Benevides [a], Alana F. Pires [c], Albertina A.S. Sousa [c], Luis A.G. Souza [d], Ana Maria S. Assreuy [c], Henri Debray [e], Walter F. de Azevedo Jr. [f], Alexandre H. Sampaio [g], Benildo S. Cavada [a,*]

[a] *BioMol-Lab, Departamento de Bioquímica e Biologia Molecular, Universidade Federal do Ceará, P. O. Box 6043, 60.455-970 Fortaleza, Ceará, Brazil*
[b] *Departamento de Biologia Molecular, Universidade Federal da Paraíba, João Pessoa, Brazil*
[c] *Instituto Superior de Ciências Biomédicas, Universidade Estadual do Ceará, Fortaleza, Brazil*
[d] *Instituto Nacional de Pesquisas da Amazônia-INPA, Manaus, Amazonas, Brazil*
[e] *Laboratoire de Chimie Biologique et Unité Mixte de Recherche N° 8576 du CNRS, Université des Sciences et Technologies de Lille, Lille, France*
[f] *Faculdade de Biociências, Centro de Pesquisas em Biologia Molecular e Funcional, PUCRS, Porto Alegre, Brazil*
[g] *Biomol-Mar, Departamento de Engenharia de Pesca, Universidade Federal do Ceará, Fortaleza, Brazil*
[h] *Program de Pós-Graduação em Química e Biotecnologia, Universidade Federal de Alagoas, Maceió, Brazil*

ARTICLE INFO

Article history:
Received 7 December 2010
Accepted 14 January 2011
Available online 26 January 2011

Keywords:
Mannose-specific lectin
Inflammation
X-ray crystallography

ABSTRACT

Legume lectins, despite high sequence homology, express diverse biological activities that vary in potency and efficacy. In studies reported here, the mannose-specific lectin from *Cymbosema roseum* (CRLI), which binds N-glycoproteins, shows both pro-inflammatory effects when administered by local injection and anti-inflammatory effects when by systemic injection. Protein sequencing was obtained by Tandem Mass Spectrometry and the crystal structure was solved by X-ray crystallography using a Synchrotron radiation source. Molecular replacement and refinement were performed using CCP4 and the carbohydrate binding properties were described by affinity assays and computational docking. Biological assays were performed in order to evaluate the lectin edematogenic activity. The crystal structure of CRLI was established to a 1.8 Å resolution in order to determine a structural basis for these differing activities. The structure of CRLI is closely homologous to those of other legume lectins at the monomer level and assembles into tetramers as do many of its homologues. The CRLI carbohydrate binding site was predicted by docking with a specific inhibitory trisaccharide. CRLI possesses a hydrophobic pocket for the binding of α-aminobutyric acid and that pocket is occupied in this structure as are the binding sites for calcium and manganese cations characteristic of legume lectins. CRLI route-dependent effects for acute inflammation are related to its carbohydrate binding domain (due to inhibition caused by the presence of α-methyl-mannoside), and are based on comparative analysis with ConA crystal structure. This may be due to carbohydrate binding site design, which differs at Tyr12 and Glu205 position.

1. Introduction

Depending on the administration route being used, lectins can be both anti- or pro-inflammatory [1]. It has been proposed that the anti-inflammatory effects elicited by exogenous lectins are due to competitive blocking of glycosylated selectin binding sites in the membranes of leukocytes and/or endothelial cells [1]. Several endogenous lectins are recognized among the adhesion molecules that actively participate in inflammatory responses, such as the selectins (L-, P-, and E-selectin) [2].

Legume lectins have notable sequence similarity and conservation, although their quaternary structure differs in a significant ways, showing relevant variant quaternary associations with important functional implications [3]. Point differences in the sequences and/or quaternary assembly of lectins translate into important biological differences both *in vivo* and *in vitro* such as

Abbreviations: ConA, *Canavalia ensiformis* lectin; Abu, α-aminobutyric acid; CGL, *Canavalia gladiata* lectin; CRLI, *Cymbosema roseum* lectin I (mannose-specific); CRLII, *Cymbosema roseum* lectin I (lactose-specific); DLLI, *Dioclea lehmanni* lectin; ConBr, *Canavalia brasiliensis* lectin; LNLS, Laboratório Nacional da Luz Síncrotron; UECE, Universidade Estadual do Ceará.

* Corresponding author. Tel./fax: +55 85 3366 9818.
E-mail address: bscavada@ufc.br (B.S. Cavada).

0300-9084 © 2011 Elsevier Masson SAS. Open access under the Elsevier OA license.
doi:10.1016/j.biochi.2011.01.006

paw edema induction, peritoneal macrophages migration, human lymphocyte stimulation and aortic rings relaxation [4].

Legume lectins, despite of their high sequence homology, express diverse biological activities that vary in potency and efficacy.

Describing the lectins that are structurally related to *Canavalia ensiformis* seed lectin (ConA) is helpful to understanding its structural features and relationships.

ConA-like lectins are composed of (β and γ) chains which are products of a pre-pro-protein cleavage [5]. The active protein is a fused final product (α chain) in inverted order for these two smaller chains [5]. This process, named posttranslational sequence circular permutation [6], probably does not occur in all legume lectins, including those from the same species [7]. This structural issue may be important when investigating lectin biological properties.

Legume lectins are normally composed of 2 or 4 subunits, presenting a molecular mass of about 25–30 kDa, with each of them presenting a unique, highly conserved carbohydrate binding site as well as conserved metal binding sites for divalent cations (calcium and manganese). The monomers are associated by non-covalent interactions in dimers stabilized as tetramers. They are described as a rigid β-sandwich, consisting of six β sheets (back) and another (front) curved sandwich with seven β sheets, and a third small β sheet, consisting of five strands bound to the others [8–10]. The carbohydrate binding site is located in the β-sandwich concave side next to the metal binding site, and consists of diverse loops with different degrees of variability [11]. In addition to the lectin carbohydrate and metal binding sites, the ability of certain lectins to bind to specific hydrophobic compounds has been reported [12]. For lectin from *Canavalia gladiata* seeds (CGL), the interactions between legume lectins and plant metabolism molecules occur in a conserved binding site for α-aminobutyric acid (Abu) [13]. Additionally, Abu was co-purified with CGL and its presence evidenced in the crystal structure was confirmed by mass spectrometry [13].

Although well-studied, some structural aspects of legume lectins are unclear. *Cymbosema roseum* seeds have two distinct lectins classified according to carbohydrate specificity. These include mannose-specific (CRLI) [14] and lactose-specific (CRLII) lectins [7]. CRLI agglutinates rabbit erythrocytes and this activity is inhibited by mannose [14], while CRLII activity is substantial inhibited by *N*-acetyl-D-galactosamine and *N*-acetyl-D-lactosamine [7]. Lectins' effects can be reversed when they are associated with their specific binding sugars. The anti-inflammatory effects of lectins have been attributed to a competitive blocking of glycosylated selectin binding sites present in the membrane of leukocytes and/or endothelial cells [1]. It also has been demonstrated that certain glucose/mannose and *N*-acetyl-glucosamine binding legume lectins, injected intravenously, inhibit neutrophil infiltration for three experimental models of inflammation [1].

The CRLI N-terminal sequence is quite similar to other lectins purified from Diocleinae species, presenting 100% similarity to *Dioclea lehmanni* lectin (DLLI) [15] and *Canavalia brasiliensis* lectin (ConBr) [16]; and 92% to ConA [17]. The apparent molecular mass, determined by electrophoresis (SDS-PAGE), indicates three polypeptide chains of 30, 18 e 12 kDa [14]. Nevertheless, the apparent molecular mass of CRLII shows a single 25 kDa band even in reduced conditions, indicating the non-existence of β and γ chains [7]. The preliminary CRLII polypeptide chain showed only 30% similarity in comparison with mature lectins such as ConA [17]. In addition, the CRLII partial sequence exhibits 47% similarity with the ConA-like pre-translational precursor. (CAA25787) [7,18]. Comparative studies of CRLI and CRLII with ConA may help to explain the differences in carbohydrate protein recognition in despite of high gene homology or sequence similarity. A greater understanding of this will improve the biotechnological potential of these lectins, but glycans co-crystallization may be required to characterize these differences.

The present study explores the structural/functional relationship of CRLI using X-ray crystallographic analysis and the evaluation of the lectins comparative effects on acute inflammation.

2. Material and methods

2.1. Protein purification

Isolation and purification of CRLI was performed by mannose affinity chromatography [14]. *C. roseum* seeds were ground to a fine powder in a coffee mill. The powder was mixed with 0.15 M NaCl (1:10, w/v) at room temperature for 4 h and centrifuged at 10,000 × g for 20 min at 278 K. The resultant supernatant was applied to a Sepharose-4B-mannose column equilibrated with a solution of 0.15 M NaCl, 5 mM $CaCl_2$ and 5 mM $MnCl_2$. After removing the unbound material, the lectin was eluted with 0.1 M glycine, 0.15 M NaCl, pH 2.6. The eluted sample was exhaustively dialyzed against water and lyophilized. Purified CRLI was monitored by SDS-PAGE and was analyzed by mass spectrometry and used in crystallization trials and carbohydrate affinity tests.

2.2. Enzymatic digestion and protein sequencing

CRLI (1 mg) was dissolved in 100 mM ammonium bicarbonate, mixed with 25 μL of 2 mg/mL bovine pancreatic trypsin (Sigma–Aldrich) and incubated for 3 h at 310 K. CRLI was also dissolved in 100 mM ammonium bicarbonate pH 8.6 and digested with endoproteinase Asp N (Sigma–Aldrich) from *Pseudomonas fragi* for 8 h at 310 K. Another CRLI sample was dissolved in 50 mM Tris–HCl pH 8.0 and digested with Glu C (Sigma–Aldrich) from *Staphylococcus aureus* for 16 h at 298 K. The enzyme: substrate ratio for Asp N and Glu C was 1:50 and 1:20 (w/w), respectively. All reaction mixtures were centrifuged at 13,000 × g for 10 min and the supernatants dried in a Speed-Vac. The peptides were loaded on a reversed-phase HPLC C18 column (5 μm particle size) and eluted at 1 mL/min with a gradient of 0.1% trifluoroacetic acid in water (solution A) and acetonitrile (solution B). The gradient was formed with a 5% of solution B for 5 min, followed by 5–40% of solution B for 60 min, and finally 40–70% of solution B for 20 min. The digested peptide samples isolated by reverse phase chromatography were diluted 100× with Milli-Q™ water, injected into a nano-electrospray ionization source and analyzed in Micromass™ quadrupole time of flight instrument from Waters™ (Massachusetts, USA) with a resolution of 8000 and an accuracy of 10 ppm. The data were processed using the manufacturer's Biolynx 4.0 program. The peptides were sequenced by ProteinLynx (Micromass™) and MASCOT (Matrix Science™) programs by *DeNovo* Sequencing and MS/MS Ion Search, respectively. Alignment and phylogenetic analysis of the CRLI sequence, with non-redundant proteins, deposited in the National Center of Biotechnology Information (NCBI), were performed by ESPript [19] and BLAST. Leucine and isoleucine were distinguished by aligned sequences based on the high similarity to ConA-like lectins.

2.3. Crystallization and X-ray data collection

The purified CRLI was dissolved at a concentration of 12 mg mL^{-1} in 10 mM Tris–HCl pH 8.0, 0.5 mM $CaCl_2$ and 0.5 mM $MnCl_2$ for use in crystallization trials. Crystallization was performed, as referred to previously by Cavada and co-workers [14], using the hanging-drop vapor-diffusion method in Linbro™ plates at 293 K. Drops were composed of equal volumes (2 μL) of both protein and reservoir solutions and were equilibrated against 500 μL of reservoir solution.

The crystals were grown in 0.1 M Tris–HCl pH 7.8, containing 8% (w/v) polyethylene glycol (PEG) 3350 and 0.2 M proline. Crystals were transferred to a cryoprotectant solution consisting of 30 % glycerol and 70 % reservoir solution. Data were collected at 100 K temperature, using 1.42 Å wavelength at beamline MX1 station (Laboratório Nacional da Luz Síncrotron – LNLS, Campinas, Brazil), using a CCD (MAR research) imaging plate at 70 mm from the crystal. A set of 120 images (1° oscillation) was recorded. Diffraction data were indexed, integrated and scaled using MOSFLM [20] and SCALA [21].

2.4. Protein structure determination

The structure was solved by molecular replacement with AMoRe [21] using the monomeric structure of ConA (PDB 1CJP) [22]. Crystallographic refinement was carried out by cycles of maximum likelihood refinement with Refmac 5 [21].

First, a detailed rigid body refinement was performed to verify the relative position of CRLI rigid groups. Afterwards, restrained refinement and corrections and/or substitutions of amino acid side chains were made using the Fo–Fc electron density map generated and visualized by Coot [23]. Water molecules were added by Coot and inspection was carried by difference Fourier maps and stereochemical criteria. Finally, an anisotropic refinement was developed and the quality of the CRLI model was checked by the Procheck program [21]. Visualization was carried out by Coot [23] and Pymol [24]. Atomic coordinates for the *C. roseum* lectin crystal structure have been deposited in the Protein Data Bank, (code 3A0K). The PDB code for the proteins used in the analysis is 1CJP for ConA (Hamodrakas et al., 1997) [22]. An omit map was built using the Omit program; a Selfcheck tool [21].

2.5. Molecular docking

α-D-mannosyl-1,3-α-D-mannosyl-1,6-α-D-mannopyranoside was used to verify the carbohydrate binding properties of CRLI. The coordinates of the glycans were generated by Sweet II and the choice of the ligand was made based on affinity assays. Molecular docking analysis was performed with MOLDOCK an interactive molecular graphics program [25]. MOLDOCK is an implementation search algorithm that joins together differential evolution with a cavity calculation algorithm. In the MOLDOCK, the docking scoring function is extended with an additional term, taking hydrogen bond directionality into account. In addition a re-ranking procedure is also applied in order to augment docking accuracy [26].

2.6. Affinity assays

Affinity tests were carried out based on CRLI haemagglutinating activity inhibition, using native and enzyme-treated rabbit erythrocytes; the enzymes used were papain and trypsin. Inhibition tests were carried out using monosaccharides and disaccharides (D-glucose, D-mannose, D-galactose, D-lactose, L-fucose, *N*-acetyl-D-galactosamine, *N*-acetyl-D-glucosamine and *N*-acetyl-D-lactosamine), *N*-glycoproteins (human serotransferrin, human lactotransferrin, hen ovalbumin, bovine thyroglobulin, porcine thyroglobulin, bovine lactotransferrin and desialylated bovine lactotransferrin) and O-glycoproteins (bovine fetuin, bovine asialofetuin, bovine submaxillary mucin, porcine stomach mucin, ovine submaxillary mucin and desialylated ovine submaxillary mucin). The saccharides were purchased from Sigma–Aldrich and the glycoproteins were isolated by Laboratoire de Chimie Biologique et Unité Mixte de Recherche (Université des Sciences et Technologies de Lille, France).

CRLI samples were diluted in 0.15 M NaCl to a final concentration of 4 units of haemagglutinating activity per mL. 0.2 mL of the diluted lectin (1/256) was added to 96-well plates containing the diluted inhibitors. The plates were left at room temperature for 1 h before the addition of 2 % native or enzyme-treated rabbit erythrocytes (0.2 mL). After 1 h, haemagglutination was observed by microscope. The haemagglutinating titer (210) was defined as the highest dilution of CRLI that agglutinates erythrocytes (HU mL^{-1}). The inhibition haemagglutinating titer was defined as the highest

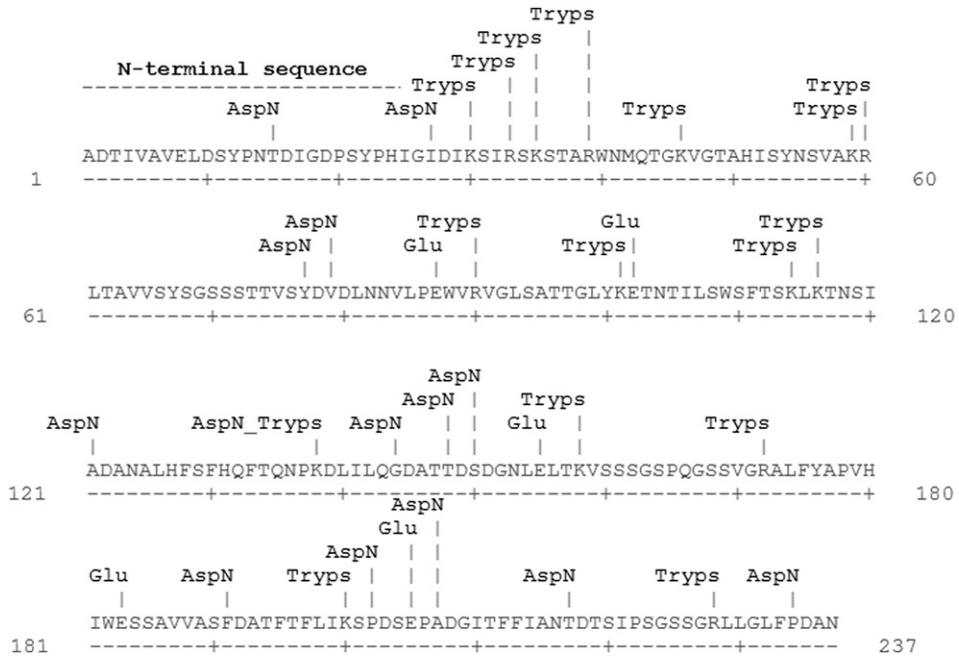

Fig. 1. Complete amino acid sequence of the CRLI determined by mass spectrometry. The N-terminal was previously sequenced by Edman's Degradation and the cleavage protease sites were assigned. The peptides sequenced by tandem mass spectrometry were obtained by enzymatic digestions of (D) endoproteinase AspN from Pseudomonas, (E) endoproteinase Glu-C or (T) trypsin. The likely positions of the digested peptides were determined based on the alignment with *D. guiansensis* seed lectin (Dgui). Leucine and Isoleucine were differed by similarity on MS/MS ion search.

dilution of inhibitor which reduced agglutination using 4 haemagglutinating units.

2.7. Biological assays

2.7.1. Animals

Male Wistar rats (150–250 g) were used. The animals were grown and housed (6 per cage) in rooms with a controlled 12/12 h light/dark cycle, at 25 °C with free access to food and water. The experimental protocols used in this study were approved by the Institutional Animal Care and Use Committee of the Universidade Estadual do Ceará (UECE N° 0559924-4), Fortaleza-CE, Brazil, in accordance with the Guide for the Care and Use of Laboratory Animals of the US Department of Health and Human Services (NIH publication n° 85-23, revised 1985).

2.7.2. Rat paw edema model

Paw volume was measured before subcutaneous (s.c.) injection of inflammatory stimuli (zero time) into the hind paw of rats and at selected time intervals (1–6, 18 and 24 h) thereafter by hydroplethysmometry. Results were expressed as the increase or reduction in paw volume (mL) calculated by subtracting the basal volume measured at zero time.

In order to evaluate the lectin edematogenic activity, paw edema was induced by (s.c.) injection of CRLI (0.01, 0.1, 1 mg/kg) in a final volume of 0.1 mL/100 g body mass and compared to a group of animals that had received the same volume of sterile saline (NaCl 0.9%). For the anti-edematogenic effect, CRLI was injected intravenously (i.v.), at the most active pro-inflammatory dose, 30 min before s.c. injection of carrageenan (300 μg/paw), a classical edematogenic agent. Positive edema controls received carrageenan s.c. and negative controls, sterile saline following the same protocol.

In order to evaluate the inhibition of both pro- and anti-inflammatory CRLI effects by carbohydrates, a solution containing the most active dose of lectin associated to its specific ligand, α-methyl-D-mannoside (α-CH3 −0.1 M), was incubated during 60 min at 37 °C to allow binding between lectin and sugar before injection (s.c. or i.v.) into animals.

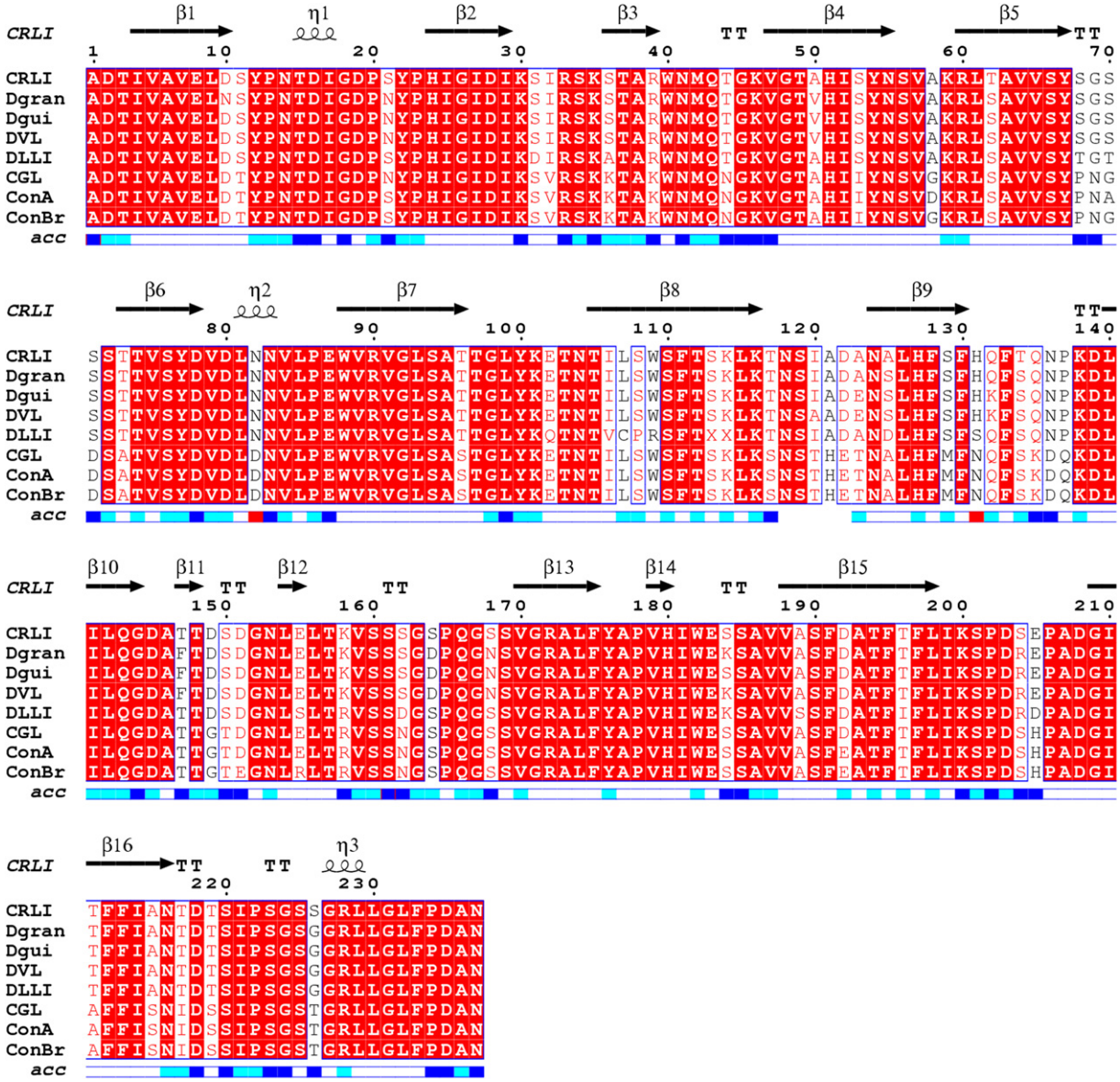

Fig. 2. Multiple sequence alignment of CRLI sequence obtained by mass spectrometry with the seed lectins of *Dioclea grandiflora* (Dgran), *D. guianensis* (Dgui), *D. violacea* (DVL), *D. lehmani* (DLLI), *Canavalia gladiata* (CGL), *C. brasiliensis* (ConBr) and *C. ensiformis* (ConA).

3. Results

3.1. Protein sequencing

The CRLI sequence (Fig. 1) is composed of 237 amino acid residues with a calculated pI = 5.1 and a molecular mass of 25,326 Da, confirmed by mass spectrometry (MALDI-ToF) (Data not shown). The sequence is highly similar to other lectins purified from the *Canavalia* and *Dioclea* genera. CRLI presents similarity with lectins from *Dioclea grandiflora* (1DGL), *Dioclea guianensis* (1H9W), *Dioclea violacea* (2GDF), *Canavalia gladiata* (2D7F), *Canavalia ensiformis* (1CJP) and *Canavalia brasiliensis* (1AZD) at 97%, 98%, 96%, 92%, 92% and 91%, respectively (Fig. 2). The protein sequence reported in this paper can be found in the UniProt Knowledgebase under the accession number P86184.

3.2. Crystal structure analysis

CRLI crystals were obtained according to Cavada and co-workers [14]. The diffraction data showed that the crystals belong to the $P2_12_12_1$ space group with cell parameters at $a = 68.0$ Å; $b = 103.1$ Å and $c = 122.3$ Å. Data processing, scaling, and refinement statistics are presented in Table 1. Molecular replacement was performed using ConA crystal structure coordinates [PDB 1CJP] as the search model. A tetramer in the asymmetric unit was determined by Matthews Coefficient ($Vm = 2.1$ Å^3 Da^{-1}) [27], which indicates a solvent content of 41.9%.

The overall structure of native CRLI (Fig. 3a) has been refined to a 1.8 Å resolution. The model presents acceptable stoichiometry based on Ramachandran plot and a well-defined geometric structure. Calculated r.m.s.d shows alpha carbon deviations between CRLI and ConA of 0.28, and back bone deviations of 0.295. The main deviations are in the loops, including the loop of the carbohydrate binding domain.

3.3. Metal and carbohydrate binding sites

The amino acids involved in metal binding are conserved, and the structures of the Mn^{2+} and Ca^{2+} binding sites showed similarities with those of other legume lectins (Fig. 3b). Monomers contain manganese and calcium ions in the vicinity of the saccharide-binding site. The calcium ion coordination induces a trans-cis peptide bond isomerization between Ala207–Asp208. The manganese binding also establishes some coordination interactions to stabilize the carbohydrate binding site. Each of the metal ions is coordinated by four amino acid side chains and two water molecules: Glu8, Asp10, Asp19 and His24 with Mn^{2+}; Asp10, Tyr12, Asn14 and Asp19 with Ca^{2+}. In the case of the calcium ion, one of the water molecules forms a bridge between the metal and the main-chain carbonyl group of Asp208, stabilizing the unusual Ala207–Asp208 cis-peptide bond. The carbohydrate binding site has been widely described in ConA-like lectins, for monosaccharide interactions [28,22]. The amino acid residues of the carbohydrate binding site (Asn14, Leu99, Tyr100, Asp208 and Arg228) participate in five to eight hydrogen bonds in Diocleinae lectins [22].

A trimannoside was placed into the CRLI carbohydrate binding domain by docking and the interactions formed between the glycan and the amino acids were formed mainly by polar contacts and Van der Waals interactions. These interactions are formed by representative amino acids in the previously characterized ligand site of legume lectins (Asn14, Asp208 and Arg228), and are also formed by some residues which compose the extended trimannoside binding site (Thr15, Asp16, Ser226 and Gly227) (Table 2) (Fig. 4). Van der Waals contacts are established between hydrophobic sub-site amino acids (Tyr12 and Leu99) and the central mannose of glycan (Table 2), and other interactions can be observed involving Asn14, Asp16, Ser226 and Gly227 totaling nine Van der Walls contacts. The trimannoside chosen for docking calculations is a core to *N*-glycoproteins which inhibited CRLI with high specificity (View Table 3). The docking results corroborate with affinity assays displayed bellow.

Table 1
Statistics of data collection, refinement and structure quality.

Parameters	Values
Data collection	
Beamline wavelength	1.42 Å
Space group	$P2_12_12_1$
Exposure time per frame (sec)	100
Mosaicity	0.69
Unit cell parameters (Å)	
a	67.82
b	103.14
c	122.09
Total reflections	289,573
Number of unique reflections	78,957
Molecules per Asymmetric Unit	Tetramer
Resolution Limits (Å)	34.92–1.8
R_{merge}[b] (%)	5.5 (28.1)[a]
Completeness (%)	94.9 (98.3)[a]
Multiplicity	3.7
I/σ (Average)	11.8 (2.4)[a]
Molecular replacement	
Correlation coefficient	73.4
R_{factor}[c] (%)	34.0
Refinement	
Resolution range (Å)	34.92–1.8
R_{factor}[c](%)	18.4
R_{free}[d] (%)	23.5
Number of residues in asymmetric unit	948
Number of water molecules	705
Temperature factors (Å^2)	
Wilson *B* Factor	14.9
Average *B* value for whole protein chain	15.19
RMS deviations	
Bond length (Å)	0,016
Bond angle (degree)	2,012
Ramachandran plot	
Residues in most favored regions (%)	96.3 %
Residues in additional allowed regions (%)	3.5 %
Residues in generously allowed regions (%)	0.2 %

[a] Values in parenthesis represent the high resolution shell (1.9–1.8 Å).
[b] $R_{merge} = (\sum_{hkl}\sum_i |\bar{I}(hkl) - \langle I(hkl)i\rangle|)/(\sum_{hkl}\sum_i \langle I(hkl)i\rangle)$ where *I(hkl)i* is the intensity of *i*th measurement of the reflection h and *I(hkl)* is the mean value of the *I(hkl)i* for all I measurements.
[c] $R_{factor} = (|F_{obs}| - |F_{calc}|)/|F_{obs}|$.
[d] Calculated with 5% of the reflections omitted from refinement.

3.4. α-aminobutyric acid (Abu) hydrophobic pocket

In addition to the carbohydrate and metal binding sites, legume lectins have a hydrophobic α-aminobutyric acid (Abu) pocket [13]. Abu was co-purified with CRLI in the same way as previously reported for CGL. The observation of this molecule was first evidenced by Fo–Fc map analysis. It was observed that the molecule was the same as reported by this previous work and that the orientation and interactions with protein structure were the same. After refinement, the Abu electron density was confirmed in 2Fo–Fc map and an omit map was generated and confirmed the evidence (Fig. 5).

This pocket is also visible in the CRLI crystal structure, and is located within the monomer interfaces of canonical dimers. The residues involved in this interaction are highly conserved and the

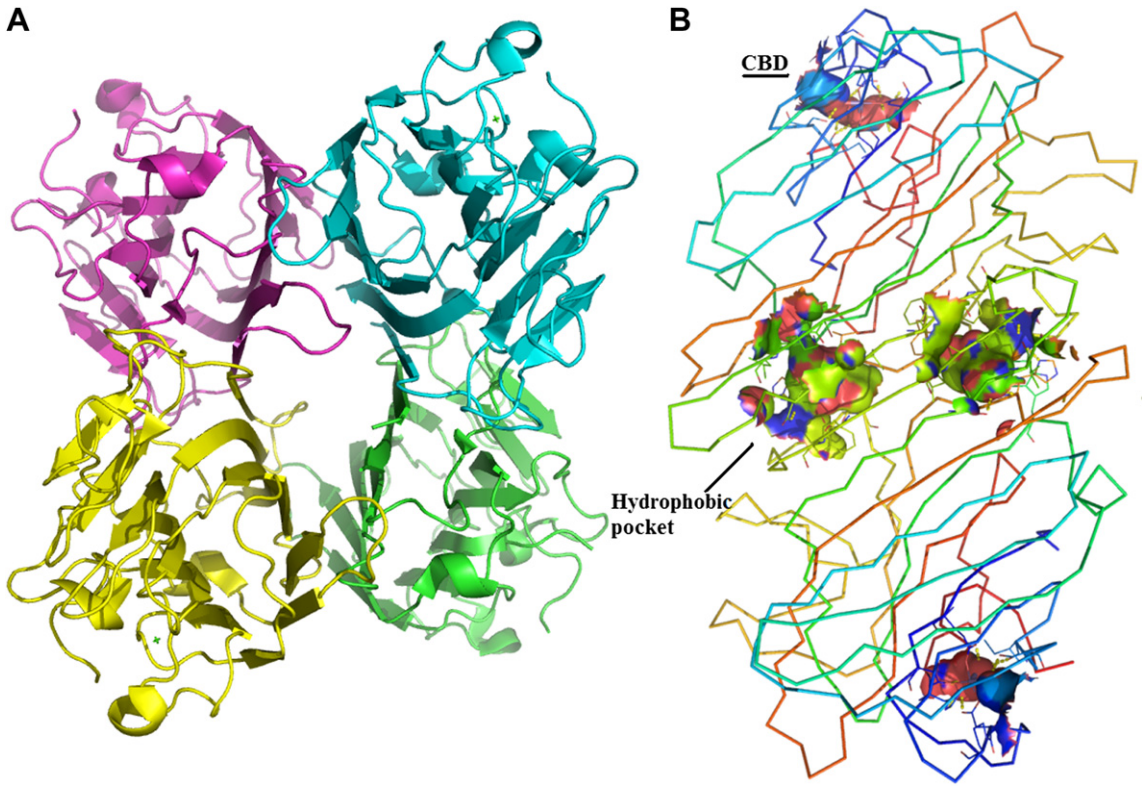

Fig. 3. CRLI overall crystal structure. (A) Tetrameric assembly of CRLI as dimer of canonical dimers. (B) Ligand sites: Carbohydrate binding domain (CBD) stabilized by metal biding loop coordination and the hydrophobic pocket.

position of the ligand molecule is very similar to that found in CGL (PDB code 2D7F) [13]. Abu, a non-protein amino acid involved in plant response against pathogens [29], is accessible to the solvent surface and on binding to the protein forms hydrogen bonds with the side chain of Asp139 and a water molecule mediated hydrogen bond with the side chain of Asn124. In the other canonical dimer's chain, the interaction is made by hydrogen bond with Ala125 and another water molecule interacting with His180 (Fig. 6). Abu also forms hydrophobic interactions with Leu126 and Val179. The term "hydrophobic pocket" refers to the hydrophobic interactions that orient the position of Abu in its site, and also the fact that the cavity is hydrophobic. The ABU site is positioned just at the end of this characteristic cavity, which extends across the entire canonical dimer of CRLI.

A 2.75 Å hydrophilic interaction occurs between Abu and Asp139 and involves the OD2 oxygen from Asp139 hydroxyl group and the Abu oxygen. The same Abu oxygen forms a 2.6 Å hydrogen bond with a water molecule, and the Abu nitrogen also interacts with another water molecule.

The interactions and stabilization caused by Abu, at the dimers interface, reduces vibrational forces and permits a more correct positioning of the amino acids main chain of loop 117–123 in the CRLI crystal structure. This is evidenced by the electron density observed for this loop, which is commonly absent in other related structures, such as ConA crystal structures.

Table 2
Main interactions between trimannoside and carbohydrate binding domain of CRLI.

Amino acid	Carbohydrate	Distance (Å)
Hydrogen bonds		
Thr15-OG1	M1-O2	3.0
Asp16-OD1	M1-O3	2.4
Asn14-ND2	M2-O2	2.8
Asn14-ND2	M2-O3	2.8
Asp208-OD1	M2-O2	2.7
Asp208-OD2	M2-O2	3.4
Arg228-NH1	M2-O4	3.2
Ser226-O	M3-O3	2.7
Ser226-OG	M3-04	3.0
Ser226-O	M3-04	3.0
Gly227-N	M3-O4	2.4
Van der Waals interactions		
Tyr12-CE2	M2-CH1	2.8
Tyr12-CE2	M2-CH6	3.0
Tyr12-CE2	M2-OR	2.5
Leu99-CD2	M2-O1	3.0

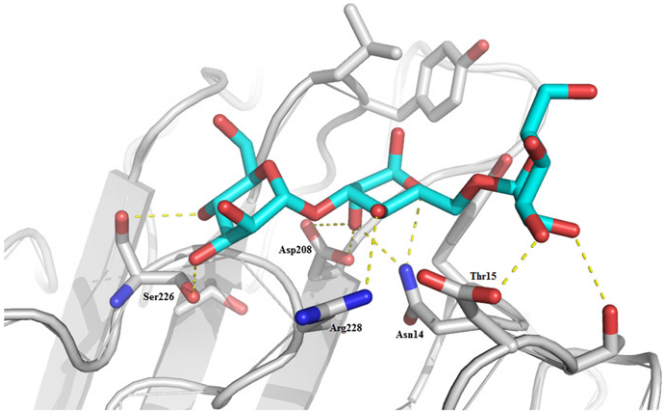

Fig. 4. H-bonds formed between CRLI and trimannoside core calculated by docking. The amino acid forming polar contacts are Asn14, Thr15, Asp16, Asp208, Ser226 and Arg228.

Table 3
Glycan structures of glycoproteins used in inhibitory assays.

	Glycan structure[a]
N-glycoprotein	
Human serotransferrin Human lactotransferrin Hen ovalbumin Bovine thyroglobulin Porcine thyroglobulin Bovine lactotransferrin Desialylated bovine lactotransferrin	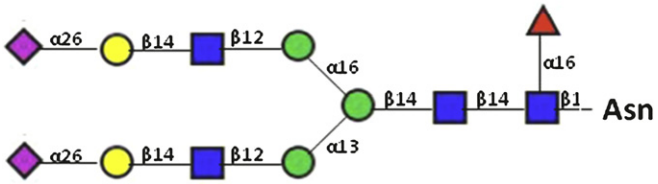
O-Glycoprotein	
Ovine submaxilar mucin	
Desialylated submaxilar mucin	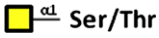 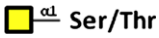 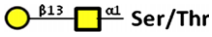
Porcine stomach mucin	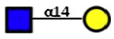 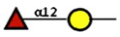 
Bovine submaxilar mucin	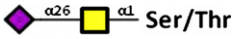  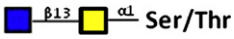 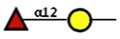 
Asialofetuin	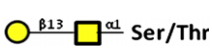

[a] Symbols: Mannose(●), Galactose (○), Glucose (●), Fucose (▲), *N*-Acetyl-Galactosamine (□), *N*-Acetyl-Glucosamine (■), *N*-Acetyl-Neuraminic Acid (◆).

3.5. Affinity and biological assays

The inhibition of haemagglutination caused by monosaccharides was mainly due to D-mannose. The glycan-recognizing specificity of CRLI was investigated using different carbohydrates and glycoproteins (structurally described in Table 3). With respect to the *N*-glycoproteins, bovine lactotransferrin, porcine thyroglobulin, and bovine thyroglobulin presented the most potent inhibitory effects at 1.2, 2.4 and 9.7 $\mu g\,mL^{-1}$, respectively; (Table 4). O-glycoproteins were not capable of inactivating the CRLI or erythrocyte binding.

CRLI (1 mg/kg) injected s.c. induced an edematogenic effect, which started at the 3rd h after injection and reached maximal effect at the 4th h (0.47 ± 0.04 mL) compared to the saline group (0.03 ± 0.03 mL). The edema decayed in the following hours, but was maintained significantly until the 24th h of development (0.12 ± 0.03 mL) (Fig. 7a). On the other hand, CRLI (1 mg/kg) injected i.v., 30 min before the s.c. injection of carragenan (1.23 ± 0.04 mL), significantly prevented (by 33 %) the carragenan-induced edema from the 3rd (0.60 ± 0.05 mL) until the 5th h (0.85 ± 0.05 mL) of its development (Fig. 8a).

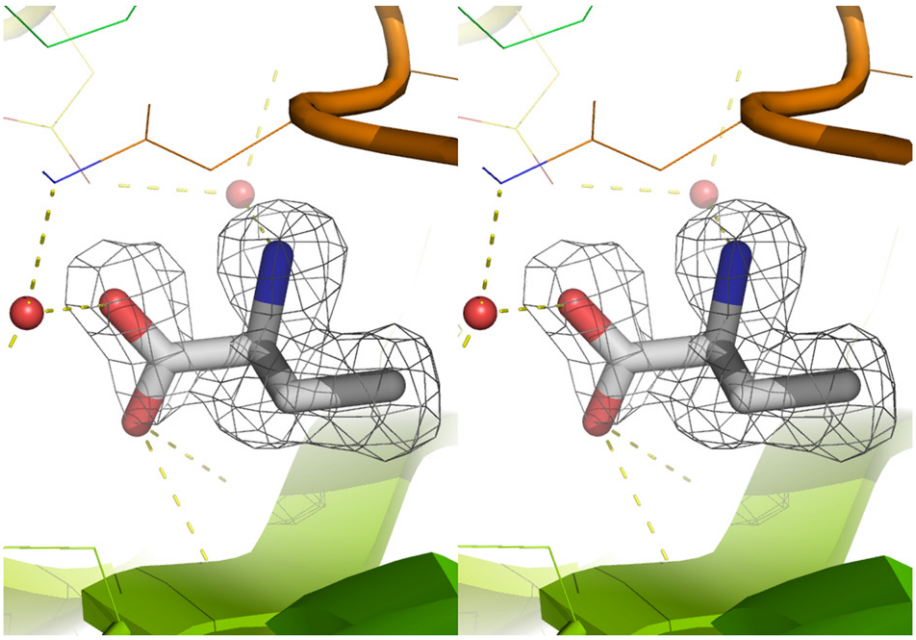

Fig. 5. Omit map well-eye stereo view representation of the α-aminobutyric acid (Abu)-Excluirbinding pocket.

The administration of lectin (1 mg/kg; s.c.) associated to its ligand sugar 0.1 M α-CH3, partially reversed (by 66%) the lectin edematogenic effect at the 4th h (0.25 ± 0.02 mL) and 5th h (0.25 ± 0.02 mL) (Fig. 7b) and completely reversed the anti-edematogenic effect at the 3rd h (1.02 ± 0.06 mL), 4th h (1.04 ± 0.06 mL) and 5th h (0.98 ± 0.04 mL) (Fig. 8b).

4. Discussion

The CRLI crystal structure solved at 1.8 A is quite similar to the jelly-roll domain commonly known to legume lectins. The quaternary structure is composed of a tetramer. The high sequence similarity and three-dimensional structure conservation are reflected in the composition and arrangement of the ligand sites. It is well established that legume lectins possess three types of hydrophobic sub sites based on different ligand affinities. The hydrophobic derivative ligands interacting with lectins, described by Kanellopoulos and co-workers [30], revealed that the hydrophobic interacting moiety is formed by Tyr12, Leu99 and Tyr100 (Fig. 9).

Dan and co-workers (1998) [31] demonstrated a core trimannoside predicted by microcalorimetric assays and suggested many interactions between methyl-mannoside which compose several deoxy-oligosaccharides. The interactions were mainly favored by approximation of central mannose to the hydrophobic sub-site. These interactions were reduced compared with CRLI interaction with a non-methylated trimannoside (Table 2) but polar contacts maintained the conserved arrangement previously suggested by Dan and co-workers [31]. The interference of methylation of disaccharides and the molecular basis of this interaction were purposed and demonstrated by Bezerra and co-workers [32].

It has been demonstrated that the affinity of ConA-like lectins for disaccharides could be explained by the H-bond between Tyr12 and the second carbohydrate moiety, possibly due to the

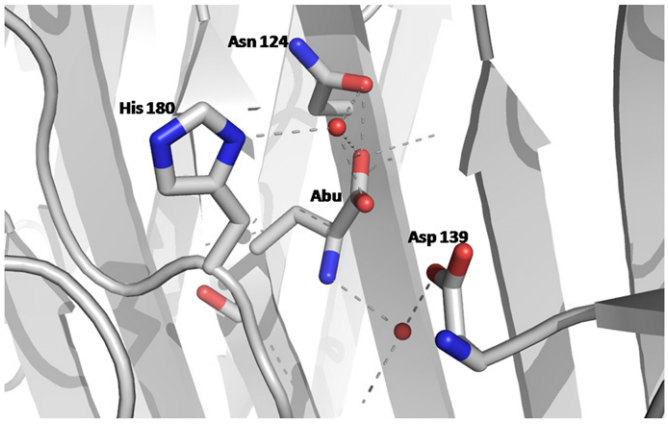

Fig. 6. Abu ligand site. H-bonds stabilize the Abu in the pocket after the anchoring by hydrophobic interactions. Asp139 from one chain and Ala125 from the other monomer chain interact with Abu by H-bonds. Two interstitial water molecules (red balls) form H-bonds with the amino and carboxyl groups of Abu. The hydrophobic contacts are established by Abu and Leu126 and Val179 from the same chain (For interpretation of the references to color in this figure legend, the reader is referred to the web version of this article.).

Table 4
Inhibition of haemagglutation by saccharides and glycoproteins of the mannose-specific lectin CRLI from *Cymbosema roseum*.

	Minimal inhibition concentration
Saccharides	*mM*
D-Mannose	37.5
L-Fucose	>75
D-Glucose	>75
N-Acetyl D-glucosamine	>75
D-Galactose	>75
D-Lactose	>75
N-Acetyl-D-lactosamine	>75
N Acetyl D-galactosamine	>75
N-glycoproteins	*μg/mL*
Bovine lactotransferrin	1.2
Porcine thyroglobulin	2.4
Bovine thyroglobulin	9.7
Human serotransferrin	156.2
Human lactotransferrin	312.5
Hen ovalbumin	312.5

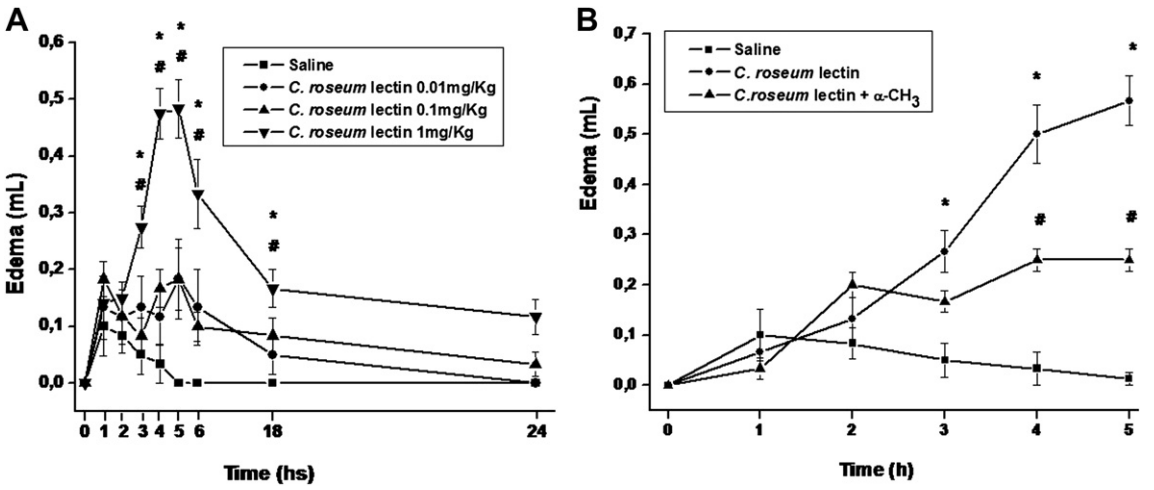

Fig. 7. Local injection of CRLI induces paw edema which is reversed by α-methyl-D-mannoside. CRLI (0.01, 0.1 and 1 mg/kg; s.c.) alone (a), or CRLI (1 mg/kg; s.c.) associated to 0.1 M α-methyl-D-mannoside (b). Negative control received sterile saline (0.1 mL/100 g body weight; s.c.). Mean ± S.E.M. ($n = 6$). *$p < 0.05$ compared to Saline; #$p < 0.05$ compared to *C. roseum* lectin.

substitution of Pro202 by Ser202. This increases significantly the lectin carbohydrate-binding capacity by reducing the interference of His205 which is closer to Tyr100 than Tyr12. Histidine-205 exhibits influence in the conformation acquired by disaccharides interacting with ConA. His205 has a "turned down" conformation in ConA, reaching Tyr12, but when His205 presents a "turned up" conformation reaching Tyr100 the interaction pattern can change significantly. CRLI presents Glu205 instead His205, but the side chain conformation is "turned up" and is closer to Tyr100 but the interference on the sub site conformation caused by a Glu205 is lower than His205. The amino acid substitution and conformation of Glu205 represents a reduction of stereochemistry conflict and causes an approximation among Tyr12, Tyr100 and Leu99 and the second mannose, maximizing the Van der Waals and hydrophobic interactions between the lectin and carbohydrate ligand (Table 2). The trisaccharide binding site in CRLI is demonstrated by docking calculations and shows the features of dimannoside interaction and characterizes an extended contact area with the ligand revealing other residues involved in carbohydrate recognition (Fig. 4). The interaction is similar to those found in ConA and DGran but not the same because the previous studies were made with methylated trimannoside, which enhances the affinity of glycans and lectins. The interactions between trimannoside and CGL and DGran differs from CRLI mainly in non-polar contacts between Tyr12, Leu99 and Tyr100, which are possible due to methyl groups that permit Van der Waals interactions and induces an approximation of these three residues and the trisaccharide.

Similar to histidine in other ConA-like lectins, Glu205 orientation probably provokes conformational changes in the active site, favoring a particular interaction mode with glycans involved in inflammatory processes (Fig. 9). This supports the hypothesis that CRLI can act as an anti-inflammatory modulator.

CRLI presented haemagglutinating activity for native and enzyme-treated rabbit erythrocytes at a minimal purified protein concentration ($<2\ \mu g\ mL^{-1}$). CRLI had more affinity to *N*-glycoproteins and CRLII, a lactose-specific lectin from *C. roseum*, was inhibited by desialylated *N*-glycoprotein (bovine lactotransferrin) at only $2.4\ \mu g\ mL^{-1}$, while the O-glycoproteins from mucin origin (bovine submaxillary, porcine stomach and desialylated ovine submaxillary) showed the most potent inhibition at a minimum concentration of $1.2\ \mu g\ mL^{-1}$ [7]. The desialylated bovine lactotransferrin was 2-fold less inhibitory compared to the

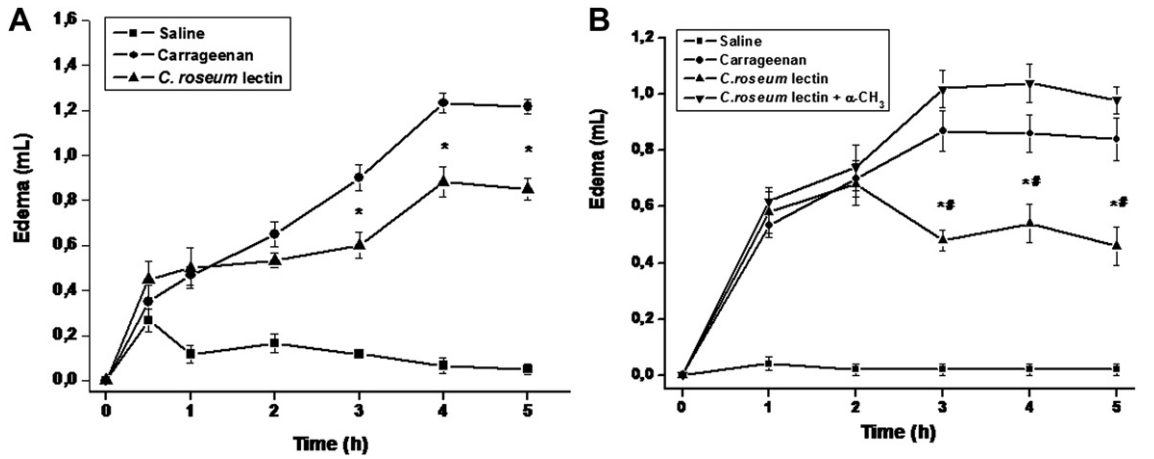

Fig. 8. CRLI inhibits the paw edema evoked by carragenan which is reversed by α-methyl-D-mannoside. CRLI (1 mg/kg; i.v.) was administered 30 min before carragenan (300 μg/paw; s.c.) alone (a), or associated to 0.1 M α-methyl-D-mannoside (b). Negative control received sterile saline (0.1 mL/100 g body weight; s.c.). Mean ± S.E.M. ($n = 6$). *$p < 0.05$ compared to carragenan; #$p < 0.05$ compared to CRLI +α-CH3.

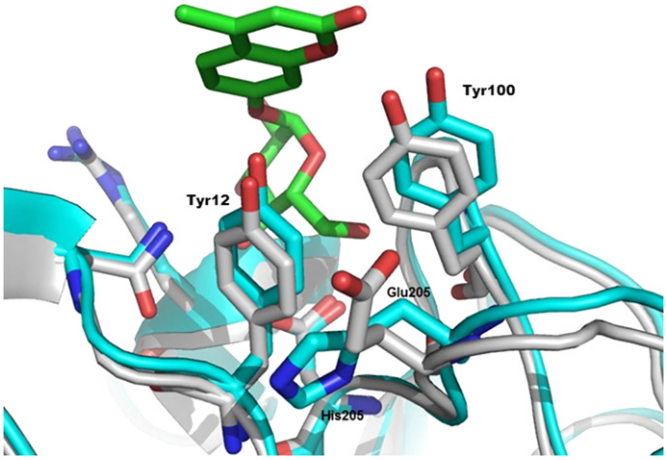

Fig. 9. Carbohydrate binding site structure alignment of ConA-like lectins. CRLI (gray) structure alignment with ConA (blue) complexed with 4-methylumbelliferyl-α-D-glucose (green) (PDB code: 1CJP). The "turned up" conformation of Glu205 (CRLI) contrasts with "turned down" conformation of His205 (ConA) and maintains the same hydrophobic sub site orientation in both molecules (For interpretation of the references to color in this figure legend, the reader is referred to the web version of this article.).

O-glycoproteins to CRLII and of the intact bovine lactotransferrin to CRLI. These differences were attributed to significant differences in primary sequence among members of a monophyletic group of Phaseoleae lectins. In this group, the synapomorphy is characterized by the carbohydrate binding property and the posttranslational process that seems to be plesiomorphic. Lectins belonging to this internal group show the posttranslational process that produces a polypeptide chain (α) composed of two smaller chains (β and γ). Based on affinity, CRLI is a potential selectin carbohydrate recognition competitor which can interfere in the adhesion process during inflammation due to its specificity for mannose-containing glycans.

The present data demonstrates that the CRLI effect in the inflammation model of paw edema is dependent on the administration route used, showing pro-inflammatory effects when by local injection and anti-inflammatory effects when by systemic injection. The involvement of the lectin domain is suggested in the CRLI effect, since both pro- or anti-edematogenic activities were reversed by the association of lectin with its binding sugar.

CRLI inhibited the inflammatory response by a competitive blocking with a common selectin carbohydrate ligand. Common carbohydrates that are able to bind selectins are N-glycans synthesized through a core structure composed of mannose and glucose [33]. These complex glycans are directly related to inflammatory processes [34]. Membrane N-glycans structures are usually involved in that response. Based on the affinity assays, CRLI has a potent ability to bind N-glycans with antennary neuraminic acid α-linked to the triantennary N-glycans core.

The crystal structure reveals some interesting features of CRLI indicating that the lectin has a high affinity to complex glycans due to the interactive capacity of its carbohydrate binding site. This increase occurs because the hydrophobic sub-site and glutamic acid 205 "turned up" orientation help glycan coupling and extends the binding site. Based on quaternary assemblies, legume lectins have been classified in nine types composed of seven different dimeric interfaces [10]. The canonical dimer type is closely related to glucose/mannose binding lectins and is the most likely to bind complex glycans synthesized with a mannose core, as well as many cell surface glycans related to selectins (inflammatory processes) and mannose binding lectins (immunologic system proteins). This is probably the main explanation for how legume lectins inhibit both pro- and anti-inflammatory processes.

The CRI route-dependent effect on acute inflammation is linked to its carbohydrate binding domain. Glucose/mannose cell surface glycans are recognized in both pro- and anti-inflammatory processes (diverging in composition) through endothelial and innate immunity cells [35]. These processes can be modulated by CRLI and other legume lectins at different levels, which themselves are directly related to oligomeric assembly and carbohydrate binding site design.

5. Conclusion

X-ray crystallography, together with biological assays, indicates that CRLI acts through the same carbohydrate specificity on different cell types. The recognition of N-glycans (mannose and glucose) is determined by the CRLI quaternary structure as well as the specific position of amino acid residues which modify the carbohydrate binding site, principally the hydrophobic sub site. Calculations of a trimannoside core interacting with CRLI demonstrate an extended site stabilized by polar contacts and Van der Waals interactions. The main mechanisms of CRLI action is to compete with selectins (systemic injection) or elicit the innate immunity response (local injection), both through saccharide recognition. In order to establish the structural features of carbohydrate binding, new structures complexed with glycans must be solved, which we are currently pursuing using co-crystallization.

5.1. Accession numbers

Coordinates and structure factors have been deposited in the Protein Data Bank with accession number 3A0K.

Acknowledgments

This study was partly financed by Fundação Cearense de Apoio ao Desenvolvimento Científico e Tecnológico (FUNCAP), Conselho Nacional de Desenvolvimento Científico e Tecnológico (CNPq) and Coordenação de Aperfeiçoamento de Pessoal de Nível Superior (CAPES). We also thank the Laboratório Nacional de Luz Síncrotron (LNLS), Campinas – Brazil. BSC, AHS, PD are senior investigators of CNPq. We thank David Erickson and David Harding for English language editing of the manuscript.

References

[1] A.M. Assreuy, G.J. Martins, E.E. Moreira, G.A. Brito, B.S. Cavada, R.A. Ribeiro, C.A. Flores, Prevention of cyclophosphamide-induced hemorrhagic cystitis by glucose-mannose binding plant lectins, J. Urol. 161 (1999) 1988–1993.
[2] M.P. Bevilacqua, R.M. Nelson, Selectins. J. Clin. Invest. 91 (1993) 379–387.
[3] V.R. Srinivas, G.B. Reddy, N. Ahmad, C.P. Swaminathan, N. Mitra, A. Surolia, Legume lectin family, the "natural mutants of the quaternary state", provide insights into the relationship between protein stability and oligomerization, Biochim. Biophys. Acta 1527 (2001) 102–111.
[4] B.S. Cavada, T. Barbosa, S. Arruda, T.B. Grangeiro, M. Barral-Neto, Revisiting proteus: do minor changes in lectin structure matter in biological activity? Lessons from and potential biotechnological uses of the Diocleinae subtribe lectins, Curr. Prot. Pep. Sci. 2 (2001) 123–135.
[5] B.A. Cunningham, J.J. Hemperly, T.P. Hopp, G.M. Edelman, Favin versus concanavalin A: circularly permuted amino acid sequences, Proc. Natl. Acad. Sci. U.S.A. 76 (1979) 3218–3222.
[6] D.M. Carrington, A. Auffret, D.E. Hanke, Polypeptide ligation occurs during post-translational modification of concanavalin A, Nature 313 (1985) 64–67.
[7] B.A. Rocha, F.B. Moreno, P. Delatorre, E.P. Souza, E.S. Marinho, R.G. Benevides, J.K. Rustiguel, L.A. Souza, C.S. Nagano, H. Debray, A.H. Sampaio, W.F. de Azevedo, B.S. Cavada, Purification, characterization, and preliminary X-ray diffraction analysis of a lactose-specific lectin from *Cymbosema roseum* seeds, Appl. Biochem. Biotechnol. 152 (2009) 383–393.
[8] K.D. Hardman, C.F. Ainsworth, Structure of concanavalin A at 2.4 A resolution, Biochemistry 11 (1972) 4910–4919.

[9] J.W. Becker, G.N. Reeke Jr., J.L. Wang, B.A. Cunningham, G.M. Edelman, The covalent and three-dimensional structure of concanavalin A, J. Biol. Chem. 250 (1975) 1513–1524.
[10] K.V. Brinda, N. Mitra, A. Surolia, S. Vishveshwara, Determinants of quaternary association in legume lectins, Protein Sci. 13 (2004) 1735–1749.
[11] V. Sharma, A. Surolia, Analyses of carbohydrate recognition by legume lectins: size of the combining site loops and their primary specificity, J. Mol. Biol. 267 (1997) 433–445.
[12] G.M. Edelman, J.L. Wang, Binding and functional properties of concanavalin-A and its derivatives. 3. Interactions with indoleacetic-acid and other hydrophobic ligands, J. Biol. Chem. 253 (1978) 3016–3022.
[13] P. Delatorre, B.A.M. Rocha, E.P. Souza, T.M. Oliveira, G.A. Bezerra, F.B. Moreno, B.T. Freitas, T. Santi-Gadelha, A.H. Sampaio, W.F. Azevedo Jr., B.S. Cavada, Structure of a lectin from *Canavalia gladiata* seeds: new structural insights for old molecules, BMC Struct. Biol. 7 (2007) 52–60.
[14] B.S. Cavada, E.S. Marinho, E.P. Souza, R.G. Benevides, P. Delatorre, L.A. Souza, K.S. Nascimento, A.H. Sampaio, F.B. Moreno, J.K. Rustiguel, F. Canduri, W.F. De Azevedo Jr., H. Debray, Purification, partial characterization and preliminary X-ray diffraction analysis of a mannose-specific lectin from *Cymbosema roseum* seeds, Acta Crystallogr. F 62 (2006) 235–237.
[15] G. Perez, M. Hernandez, E. Mora, Isolation and characterization of a lectin from the seeds of *Dioclea lehmanni*, Phytochemistry 29 (1990) 1745–1749.
[16] R.A. Moreira, B.S. Cavada, Lectin from *Canavalia brasiliensis* (MART.). Isolation, characterization and behavior during germination, Biol. Plantarum 26 (1984) 113–120.
[17] D.R. Hague, Studies of storage proteins of higher plants, Plant. Physiol. 55 (1975) 636–642.
[18] J.H. Naismith, R.A. Field, Structural basis of trimannoside recognition by concanavalin A, J. Biol.Chem. 271 (1996) 972–976.
[19] P. Gouet, E. Courcelle, D.I. Stuart, F. Metoz, ESPript: multiple sequence alignments in PostScript, Bioinformatics 15 (1999) 305–308.
[20] A.G.W. Leslie, Joint CCP4 + ESF-EAMCB, Newslett. Protein Crystallogr. 26 (1992).
[21] Collaborative computational program, The CCP4 suite: programs for protein crystallography, Acta Crystallogr. D 50 (1994) 760–763.
[22] S.J. Hamodrakas, P.N. Kanellopoulos, K. Pavlou, P.A. Tucker, The crystal structure of the complex of concanavalin A with 48-methylumbelliferyl-α-D-glucopyranoside, J. Struct. Biol. 118 (1997) 23–30.
[23] P. Emsley, K. Cowtan, Coot: model-building tools for molecular graphics, Acta Crystallogr. D 60 (2004) 2126–2132.
[24] W.L. Delano, The Pymol Molecular Graphics System. DeLano Scientific, San Carlos, CA, 2002.
[25] R. Thomsen, M.H. Christensen, MolDock: a new technique for high-accuracy molecular docking, J. Med. Chem. 49 (2006) 3315–3321.
[26] W.F. De Azevedo Jr., MolDock applied to structure-based virtual screening, Curr. Drug Targets 11 (2010) 327–334.
[27] B.W. Matthews, Solvent content of protein crystals, J. Mol. Biol. 33 (1968) 491–497.
[28] Y. Bourne, A. Roussel, M. Frey, P. Rougè, J.C. Fontecilla-Camps, C. Cambillau, Three-dimensionnal structures of complexes of *Lathyrus ochrus* isolectin I with glucose and mannose: fine specificity of the monosaccharide-binding site, Prot. Struct. Func. Gen. 8 (1990) 365–376.
[29] J. Ton, B. Mauch-Mani, γ-amino-butyric acid-induced resistance against necrotrophic pathogens is based on ABA-dependent priming for callose, Plant J. 38 (2004) 119–130.
[30] P.N. Kanellopoulos, K. Pavlou, A. Perrakis, B. Agianian, C.E. Vorgias, C. Mavrommatis, M. Soufi, P.A. Tucker, S.J. Hamodrakas, The crystal structure of the complexes of concanavalin A with 40-nitrophenyl-alpha-D-mannopyranoside and 40-nitrophenyl-alpha-D-glucopyranoside, J. Struct. Biol. 116 (1996) 345–355.
[31] T.K. Dam, S. Oscarson, J.C. Sacchettini, C.F. Brewer, Differential solvation of "Core" trimannoside complexes of the *Dioclea grandiflora* lectin and Concanavalin A detected by primary solvent isotope effects in isothermal titration microcalorimetry, J. Biol. Chem. 273 (1998) 32826–32832.
[32] G.A. Bezerra, T.M. Oliveira, F.B.B.M. Moreno, E.P. Souza, B.A.M. Rocha, R.G. Benevides, P. Delatorre, W.F. de Azevedo Jr., B.S. Cavada, Structural analysis of *Canavalia maritima* and *Canavalia gladiata* lectins complexed with different dimannosides: new insights into the understanding of the structure–biological activity relationship in legume lectins, J. Struct. Biol. 160 (2007) 168–176.
[33] J. Mitoma, X. Bao, B. Petryanik, P. Schaerli, J. Gauguet, S. Yu, H. Kawashima, H. Saito, K. Ohtsubo, J.D. Marth, K. Khoo, U.H. von Andrian, J.B. Lowe, M. Fukuda, Critical functions of N-glycans in L-selectin-mediated lymphocyte homing and recruitment, Nat. Immunol. 8 (2007) 409–418.
[34] R.G. Gallego, J.L.J. Blanco, C.W.E.M. Thijssen-van Zuylen, C.H. Gotfredsen, H. Voshol, J. Duus, M. Schachner, J.F.G. Vliegenthart, Epitope diversity of *N*-Glycans from bovine peripheral myelin glycoprotein P0 revealed by mass spectrometry and nano probe magic angle spinning ^{1}H NMR spectroscopy, J. Biol. Chem. 276 (2001) 30834–30844.
[35] R. Loris, I.V. Walle, H. De Greve, S. Beeckmans, F. Deboeck, L. Wyns, J. Bouckaert, Structural basis of oligomannose recognition by the *Pterocarpus angolensis* seed lectin, J. Mol. Biol. 335 (2004) 1227–1240.